



Genetic localization of epicoccamide biosynthetic gene cluster in *Epicoccum nigrum* KACC 40642

Eun Ha Choi¹ · Si-Hyung Park² · Hyung-Jin Kwon¹

Received: 5 July 2022 / Accepted: 19 July 2022 / Published Online: 30 September 2022
© The Korean Society for Applied Biological Chemistry 2022

Abstract *Epicoccum nigrum* produces epipyronone A (orevactaene), a yellow polyketide pigment. Its biosynthetic gene cluster was previously characterized in *E. nigrum* KACC 40642. The YES liquid culture of this strain revealed high-level production of epicoccamide (EPC), with an identity that was determined using liquid chromatography-mass spectrometry analysis and molecular mass search using the SuperNatural database V2 webserver. The production of EPC was further confirmed by compound isolation and nuclear magnetic resonance spectroscopy. EPC is a highly reduced polyketide with tetramic acid and mannosyl moieties. The EPC structure guided us to localize the hypothetical EPC biosynthetic gene cluster (BGC) in *E. nigrum* ICMP 19927 genome sequence. The BGC contains genes encoding highly reducing (HR)-fungal polyketide synthase (fPKS)-nonribosomal peptide synthetase (NRPS), glycosyltransferase (GT), enoylreductase, cytochrome P450, and *N*-methyltransferase. Targeted inactivation of the HR-fPKS-NRPS and GT genes abolished EPC production, supporting the successful localization of EPC BGC. This study provides a platform to explore the hidden biological activities of EPC, a bolaamphiphilic compound.

Keywords Biosynthetic gene cluster · Epicoccamide · *Epicoccum nigrum* · Gene inactivation · HR-fPKS-NRPS

Hyung-Jin Kwon (✉)
E-mail: hjink@mju.ac.kr

¹Department of Biological Sciences and Bioinformatics, Myongji University, Yongin-si, Gyeonggi-do 17058, Republic of Korea

²Department of Oriental Medicine Resources and Institute for Traditional Korean Medicine Industry, Mokpo National University, Muan-gun, Jeollanam-do 58554, Republic of Korea

This is an Open Access article distributed under the terms of the Creative Commons Attribution Non-Commercial License (<http://creativecommons.org/licenses/by-nc/3.0/>) which permits unrestricted non-commercial use, distribution, and reproduction in any medium, provided the original work is properly cited.

Introduction

Epicoccum nigrum is ubiquitous soil fungus and produces several bioactive metabolites [1]. *E. nigrum* is also well-known for its plant-associated colonization and its ecological significance is widely recognized [2]. MycoCosm genome portal of Joint Genome Institute, U.S. Department of Energy provides a deep sequencing data of *E. nigrum* cont 1108929. Separate genome sequence information of *E. nigrum* ICMP 19927 became available in National Center for Biotechnology Information (NCBI) website [3].

A special feature of the highly reducing type (HR) fungal polyketide synthase (fPKS) is that a single module equipped with three β -oxo moiety modification domains (β -ketoacylreductase, KR; β -hydroxyacyldehydratase, DH; 2-enoylreductase, ER) operates in a permutation manner to dictate the reductive modification pattern in each acetate unit incorporation step [4]. The C-methyltransfer domain of fPKS methylates the α -carbon of newcomer acetate on specific round(s) of chain elongation [4]. HR-fPKS is often found as a fusion protein with a module of nonribosomal peptide synthetase (NRPS) and a polyketide backbone terminated with a specific amino acid [5]. Chain release chemistry and subsequent chemical modifications contribute to the chemical diversity of the HR-fPKS-NRPS products.

Genome mining has become a general approach in secondary metabolite (SM) biosynthesis studies [6,7], whereas genome localization of the SM biosynthetic gene cluster (BGC) has rarely been practiced for *E. nigrum*. Orevactaene (OVT; OVT is used to avoid confusion with epicoccamide EPC, whereas previous studies employed the terminology epipyronone A/EPN-A, the synonym of orevactaene) BGC characterization is the sole case of *E. nigrum* genome mining in SM biosynthesis [8,9]. This study revealed that the public *E. nigrum* genome sequences can be readily applied in the genetic engineering of *E. nigrum* KACC 40642. Molecular genetics and subsequent biochemical experiments can be regarded as a part of BGC genome mining because they

eventually determine the relevance of BGC localization. Generally, the genome mining approach requires reliable production conditions for a particular SM. If the genome sequence is available and a high level of production is secured, the genome mining study for SM of our interest is straightforward, especially for polyketides whose biosynthetic mechanism is finely defined [10]. In this study, we identified and characterized epicoccamide (EPC) BGC in *E. nigrum* KACC 40642 using a genome mining approach, providing a platform to explore the biochemical properties of EPC, a bolaamphiphilic compound with neither antimicrobial nor cytotoxic activity.

Materials and Methods

Culture conditions, extraction methods, and analytical procedures *E. nigrum* KACC (Korean Agricultural Culture Collection) 40642 was used in this study. *E. nigrum* wild-type (WT) and its derivatives were grown on potato dextrose agar (PDA) at 25 °C for 7 d. Antifungal agent was added in PDA when necessary. Agar blocks of the PDA culture were used to initiate yeast extract sucrose broth (YES) that is composed of 4% yeast extract and 16% sucrose. The liquid cultures were prepared in 50 mL culture volume in 250 mL baffled flask and maintained at 25 °C for 7 d with a shaking speed of 250 rpm. The cell and supernatant of the resulting liquid culture were separated using centrifugation and were extracted with methanol and ethylacetate, respectively. The organic extract was dried in a reduced pressure to be dissolved in methanol for chemical analysis. TLC analysis was performed on a silica gel plate (silica gel 60 F254 TLC plates; Merck, Darmstadt, Germany) that was developed with with a mixture of *n*-butanol/acetic acid/water (12:3:5, by volume). EPC can be readily identified with its apricot color in this acidic TLC condition.

High-performance liquid chromatography (HPLC) analysis was performed on a Prostar system (Varian) with a Gemini C18 column (150×3.0 mm, particle size of 5 µm, pore size of 11 nm; Phenomenex, Torrance, CA, USA) and the elution was monitored at 260 nm. Absorbance at 330 nm was used to differentiate the EPC peak from that of OVT isomers. Absorbance of EPC at 330 nm is much lower than that at 260 nm, while the OVT signal is significantly higher at 330 nm than at 260 nm. The mobile phase consisted of 0.1% formic acid in water (A) and 0.1% formic acid in acetonitrile (B). The flow rate was maintained at 0.5 mL/min. The system was run with the following gradient program: 100% A for 5 min, from 100% A to 80% A over 10 min, from 80% A to 100% B over 10 min, then maintained at 100% B for 10 min.

Liquid chromatography (LC)-mass spectrometry (MS) analysis was performed with Dionex UltiMate 3000 UHPLC (Thermo Scientific, Sunnyvale, CA, USA) combined with LTQ XL Orbitrap mass spectrometer (Thermo Scientific, Bremen, Germany) on a reverse-phase Kinetex column (100 mm×2.1 mm, particle

size of 1.7 µm, pore size of 10 nm; Phenomenex, Torrance, CA, USA). The flow rate was maintained at 0.2 mL/min. Gradient elution was performed with the mobile phase composed of 0.1% formic acid in water (A) and 0.1% formic acid in acetonitrile (B). The LC gradient elution was applied with the following program: from 90% A to 50% A over 20 min, from 50% A to 100% B over 10 min, then maintained at 100% B for 10 min. Electrospray ionization was performed in positive-and negative-ion mode and mass spectra were obtained in Fourier-transform mode with resolution of $R=30,000$ at m/z 400.

Isolation of EPC from *E. nigrum* Δ *ovtA*

For the isolation of EPC, the Δ *ovtA* strain cultured in potato dextrose broth at 25 °C for 7 d with a shaking speed of 250 rpm. The resulting culture was used to prepare 500 mL YES media in 2-L baffled flask. The culture was maintained at 25 °C for 7 d with a shaking speed of 250 rpm. The supernatant was collected by being passed through a filter paper and extracted with the same volume of ethylacetate twice. The ethylacetate extract was concentrated in a reduced pressure to be dissolved in 10 mL of methanol. The resulting methanol solution was applied to Diaion HP-20 resin column chromatography, which was eluted with water and an increasing amount of methanol. The fractions that contained EPC were combined and concentrated to be applied to silica gel 60 (Merck, Darmstadt, Germany) chromatography, which was eluted with an increasing amount of methanol in chloroform. The eluate fractions were analyzed using TLC as aforementioned, and the EPC-fractions were collected for Nuclear magnetic resonance (NMR) analysis. Approximately 13 mg of EPC was obtained in this isolation. NMR experiments such as $^1\text{H-NMR}$, $^{13}\text{C-NMR}$, $^1\text{H-}^{13}\text{C}$ correlation spectroscopy, $^1\text{H-}^{13}\text{C}$ heteronuclear single quantum coherence (HSQC), and $^1\text{H-}^{13}\text{C}$ heteronuclear multiple bond correlation (HMBC) were conducted in pure CD_3OD (tetramethylsilane as internal standard) at 25 °C using a Bruker AVANCE 600-MHz spectrometer.

Targeted gene inactivation in *E. nigrum*

The primers that are used in this study are shown in Table 1. Polymerase chain reaction (PCR) was performed with Herculase II Fusion DNA Polymerase (Agilent, Santa Clara, CA, USA) in plasmid construction. Total DNA samples of *E. nigrum* and its derivatives were prepared using ZR fungal/bacterial DNA miniprep kit (Zymo research, Tustin, CA, USA) with the cells grown on PDA plate. The gene inactivation plasmids were prepared in pCambia1300 (GenBank accession no. AF234296.1) and neomycin phosphotransferase II gene cassette (*npIII*) was used as the selection marker. Plasmid pII99 was the source of *npIII* [11]. It is worthwhile to note that the hygromycin resistance gene in pCambia1300 is nonfunctional in fungi because its transcription is under the control of CAMV35S promoter, a plant promoter.

The EPC HR-fPKS-NRPS gene (B5807_02542, *epcA*) was

Table 1 The nucleotide oligomers used in this study. The nucleotide sequences for cloning are italicized in which restriction enzyme sites and their remnant sequences are underlined

Name	Sequence (5' to 3')	Application
2542-Up-F	<i>ATGACCATGATTACGAATTC</i> TCTCAGGTTCCAGCCGTGGCT	pKO2542
2542-Up-R	<i>GAAGAAGCGCATTAAATTAA</i> TCGGAAAGAAGATAGGCATC	pKO2542
2542-Dw-F	<i>TTAATTAA</i> ATGCGCTTCTTCCACTATCC	pKO2542
2542-Dw-R	<i>CGACGGCCAGTGCCAAGCTT</i> CAACATTGAAGTCCATCCAG	pKO2542
2542-nptII-F	<i>CTATCTTCTTTCCGATTAAT</i> ATGCCAGTTGTTCCCAGTGA	pKO2542
2542-nptII-R	<i>TAGTGAAGAAGCGCATTAA</i> GGATTACCTCTAAACAAGTG	pKO2542
2542-ch-F	GAACCCAGCCATCGAACCGT	500 bp for <i>epcA</i>
2542-ch-R	GTCTGTAGTTTCGACAGTGG	500 bp for <i>epcA</i>
del-2542-F	TCGCTACGCGGGCCAATGAA	3.2 kb for $\Delta epcA$
del-2542-R	GCCCCAGCCAGGTAGGCCGA	3.2 kb for $\Delta epcA$
2540-Up-F	<i>ATGACCATGATTACGAATTC</i> CTCTATTTC TGATCACATA	pKO2540
2540-Up-R	<i>CAAAGGCCGATGTTAATTAA</i> ACACCTTGCTTCATCGATGGC	pKO2540
2540-Dw-F	<i>TTAATTAA</i> CATCGGCCTTTGGGCTAATC	pKO2540
2540-Dw-R	<i>CGACGGCCAGTGCCAAGCTT</i> TACTTTCTTAATTCGCGACA	pKO2540
2540-nptII-F	<i>CGATGAAGCAAGTGTTAAT</i> ATGCCAGTTGTTCCCAGTGA	pKO2540
2540-nptII-R	<i>TAGCCCAAAGGCCGATGTTA</i> GGATTACCTCTAAACAAGTG	pKO2540
2540-ch-F	CAATACTATTTTTTACCAAC	1.5 kb for WT, 3.3 kb for $\Delta epcB$
2540-ch-R	CTAGGAATGATCGACTTGCA	1.5 kb for WT, 3.3 kb for $\Delta epcB$

deleted and replaced with *nptII* through homologous recombination. The gene inactivation construct (pKO2542) was prepared by connecting the *nptII* cassette between 3 kb DNA fragments upstream and downstream of B5807_02542. Both upstream and downstream fragments were obtained using PCR reactions to be cloned into the *EcoRI* and *HindIII*-digested-pCambia1300 using the In-Fusion cloning procedure (Clontech, Mountain View, CA, USA). The *PacI* restriction site was engineered at the jointing region of the two fragments. The resulting construct was linearized with *PacI* digestion and *nptII* was cloned into the *PacI* site using In-Fusion method to generate pKO2542. The size of B5807_02542 is 12 kb and pKO2542 is designed to contain 0.2 kb fragments in 5' and 3' end of B5807_02542. The same DNA connecting strategy is used to generate the inactivation construct (pKO2540) of the EPC glycosyltransferase gene (B5807_02540). The size of B5807_02549 is 1.4 kb and the internal 1.0 kb region was deleted and replaced with *nptII* in pKO2540. Each gene inactivation construct was introduced into *E. nigrum* using the *Agrobacterium* transformation technique as previously described [8].

Results and Discussion

Production of EPC in *E. nigrum* KACC 40642

The OVT biosynthesis gene cluster was previously identified in *E. nigrum* KACC 40642, and a targeted gene inactivation study

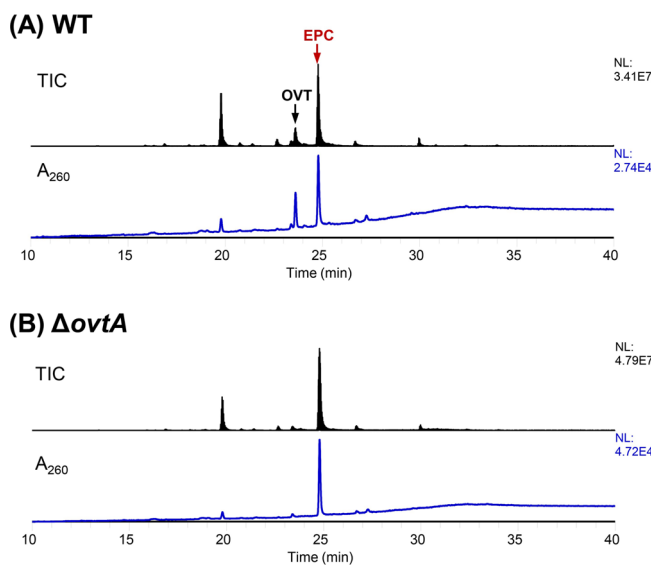


Fig. 1 LC-MS chromatograms of the organic extracts that were obtained from YES liquid cultures of *E. nigrum* KACC 40642 (A) and the $\Delta ovtA$ mutant (B). The LC-MS chromatograms of the $\Delta ovtB$ and $\Delta ovtC$ mutant were indistinguishable from that of the $\Delta ovtA$ mutant. The methanol extracts of the culture cells were used in this analysis. Total ion chromatogram (TIC) at the positive electrospray ionization and absorbance at 260 nm were shown. The eluate positions for OVT and EPC were indicated with arrows above the WT chromatogram in panel (A)

verified its role in OVT biosynthesis [8,9]. The OVT BGC is composed of three genes, *ovtA*, *ovtB*, and *ovtC*, which encode

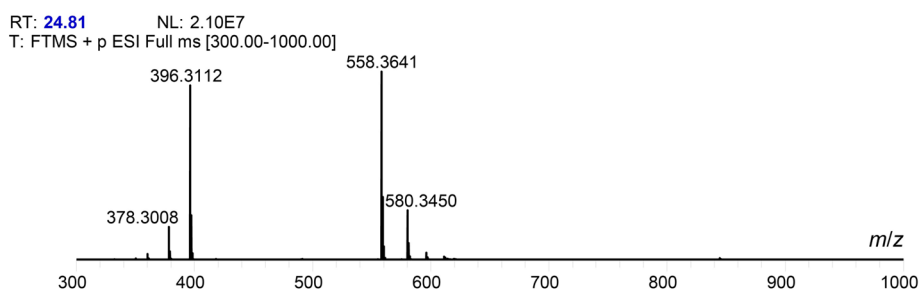
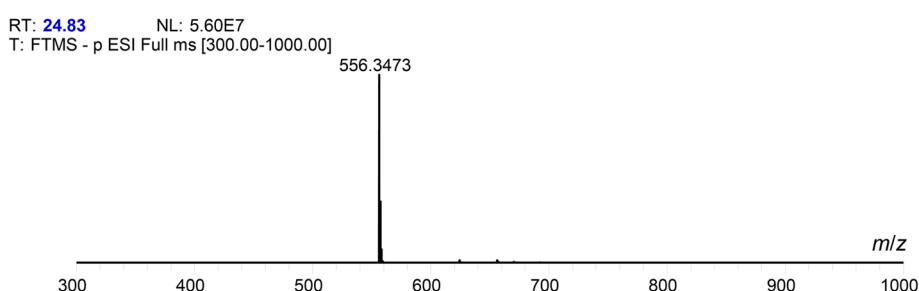
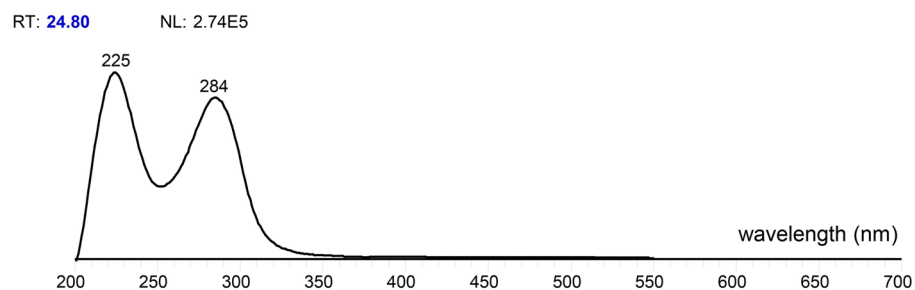
(A) positive ionization mass spectrum**(B)** negative ionization mass spectrum**(C)** UV-visible absorption spectrum

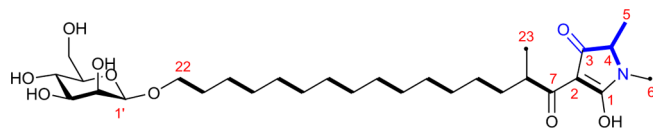
Fig. 2 Mass spectra (A, positive; B, negative) and UV-visible absorption spectrum (C) of the EPC peaks, eluted at 24.8 min in LC chromatogram of the LC-MS data in Fig. 1

HR-fPKS, glycosyltransferase (GT), and cytochrome P450, respectively. In this study, another prominent SM was found in the YES culture of *E. nigrum* KACC 40642. LC-MS analysis was conducted to assess the identity of this SM, which was eluted at 24.8 min (Fig. 1A, B). The compound was found in both the cell and supernatant extracts at a comparable level. Mass spectra showed molecular ion peaks at m/z 558.364 and 580.345 for $[M+H]^+$ and $[M+Na]^+$, respectively, in the positive ionization mode, whereas negative ionization yielded the main signal at m/z 556.347 (Fig. 2A, B). This suggested that the molecular mass of this compound was approximately 557.36 daltons. The UV-visible absorption spectrum showed absorption peaks at 225 and 284 nm (Fig. 2C).

The deduced molecular mass value was used to assess the

compound identity in the natural product library using the SuperNatural database V2 web server (https://bioinf-applied.charite.de/supernatural_new/). A molecular weight search between 557.35-557.36 provided hits for several compounds, among which one compound with the molecular formula of $C_{29}H_{51}NO_9$ (predicted molecular mass of 557.3564) was found to be a single relevant hit. The SMILES (simplified molecular-input line-entry system) information was used to search the PubChem library in NCBI server to obtain the compound name epicoccamide (EPC). EPC was first reported in *Epicoccum purpurascens* [12], which is consistent with its production in *E. nigrum*. EPC derivatives were later reported in an *Epicoccum* sp. [13]. Except for the moderate cytotoxicity and antiproliferative effects of EPC-D, no biological activity has been reported for EPCs so far [12,13]. To confirm

Table 2 ^1H (600 MHz) and ^{13}C (150 MHz) spectral data (CD_3OD) for EPC that was isolated from *Epicoccum nigrum* KACC 40462, accompanied by NMR data interpretation (text below the table)^v. The structure of EPC is shown below with carbon atom numbering



C No.	δ ^1H (ppm) (multi., J_{HH} in Hz)	δ ^{13}C (ppm)
1		176.5
2		not observed
3		197.3
4	3.50 (n.d.)	62.5
5	1.25 (n.d.)	16.1
6 (CH_3)	2.85 (br s)	26.9
7		201.9
8	3.70 (n.d.)	41.2
9	1.66 (br s), 1.20* (n.d.)	35.2
10-19	1.2-1.35 (n.d.)	30.5-31.0
20	1.36 (m)	27.3
21	1.60 (m)	30.8*
22	3.53 (td, 6.9, 9.4) & 3.90 (td, 6.7, 9.4)	69.7
23	0.94 (n.d.)	18.2
1'	4.49 (br s)	101.9
2'	3.84 (n.d.)	72.7
3'	3.44 (dd, 3.0, 9.4)	75.4
4'	3.57 (t, 9.5)	68.6
5'	3.20 (ddd, 2.2, 5.4, 9.2)	78.3
6'	3.72 (dd, 5.5, 11.8) & 3.85 (dd, 2.2, n.d.)	62.9

n.d.; not determined

*assigned with HSQC

§assigned with HMBC

^vHSQC localizes two methyl signals at 0.94 ppm (18.2 ppm δ ^{13}C) and 1.25 ppm (16.1 ppm δ ^{13}C). The former overlaps with an impurity signal, showing a COSY signal at around 3.70 ppm (8-*H*) of which ^1H signal is obscured with that of 6'-*H* and seems very broad. This 0.94 ppm ^1H signal is assigned to 23-*H* although the chemical shift is different from the published one of 23-*H* that is 1.03 ppm. Inspection of HSQC guided us to localize a weak correlation spot between approximately 3.70 ppm δ ^1H and 41.2 ppm δ ^{13}C , which is assigned to C-8. The 1.25 ppm CH_3 signal is assigned to 5-*H*. This signal is embedded in the areas of multiple signals of methylene at C-10 to -19. This 5-*H* signal shows a correlation with a broad signal at around 3.50 ppm (4-*H*) that is obscured with that of 22-*H*. HSQC identifies C-4 at 62.5 ppm with a correlation with that of 4-*H*. Lack of HMBC signals of 4-*H* and 8-*H* with the downfield carbon signals prompted us to trace HMBC signals of the methyl signals of 5-*H* and 23-*H*. 5-*H* methyl signal at 1.25 ppm shows two HMBC spots with 62.5 ppm (C-4) and 197.3 ppm, the latter of which is assigned to C-3. There is no relevant HMBC spot with the 23-*H* methyl signal. The ^{13}C signal at 201.9 ppm is thus tentatively assigned to C-7. The distinctive *N*-methyl signal at 2.85 ppm (6-*H*) shows 62.5 ppm (C-4) and 176.5 ppm, which is assigned to C-1. Other than multiple methylene signals region at 1.2-1.35 ppm, five methylene signals can be localized in HSQC. 3.72/3.85, 62.9 (ppm of proton/proton, ppm of carbon) (C-6'); 3.53/3.90, 69.7 (C-22); 1.60, 30.8 (C-21); 1.36, 27.3 (C-20); 1.20/1.66, 35.2 (C-9)

EPC production, EPC was isolated from the ΔovtA strain. The ΔovtA strain was used to avoid contamination with OVT. As shown in Table 2, the NMR measurement data of the isolated compounds are in good agreement with a previous report on EPC [12].

Genetic localization of the EPC biosynthetic gene cluster in *E. nigrum*

EPC is a mannoylated 3-acetyltetramic acid and its biosynthesis is predicted to be mediated by HR-fPKS-NRPS with the involvement of GT (Fig. 3) [5]. It is straightforward to localize the hypothetical EPC BGC in *E. nigrum* strain ICMP 19927 genome sequence (accession no. PRJNA379853) [3] because there is a single HR-fPKS-NRPS BGC in this genome, when analyzed using antiSMASH program [6]. The HR-fPKS-NRPS gene (B5807_02542; *epcA*) clusters with the genes encoding GT (B5807_02540; *epcB*), ER (B5807_02539; *epcC*), cytochrome P450 (B5807_02536; *epcD*), and *N*-methyltransferase (B5807_02535; *epcE*) (Fig. 4). The ER domain of HR-fPKS is generally non-functional, and a separate ER protein supports HR-fPKS catalysis [4]. Thus, the catalytic role of EpcC is thought to be a part of EpcA-mediated polyketide chain assembly. As depicted in Fig. 3, the acetyltetramic acid generated by EpcA is supposed to be modified by the three enzymes of EpcBDE to become EPC.

To verify the role of this BGC in the EPC biosynthesis, *epcA* and *epcB* were separately inactivated by homologous gene recombination; *epcA* and *epcB* are 12.2 and 1.4 kb, respectively. The inactivation plasmid was prepared in pCambia 1300 by amplifying two DNA fragments flanking the target genes and cloning *npIII* between them. The inactivation plasmid was introduced into *E. nigrum* using the *agrobacterium*-mediated transformation method [8]. This transformation is supposed to yield both gene replacement and whole plasmid integration mutant(s); PCR amplification was used to identify the gene replacement mutant.

In case of *epcA* inactivation, one-pot PCR for WT and ΔepcA DNA could not be achieved because of the large size of the *epcA* (Fig. 5). Thus, we adopted two separate PCR reactions, one of which showed the loss of *epcA* and the other represented the recombination of the WT chromosome and the insert of the inactivation plasmid pKO2542. The PCR primer pairs specific to *epcA* was designed to amplify 0.5 kb fragment in *epcA* (starts at 1.2 kb downstream from the start codon) and the cognate PCR indicated the absence of the 0.5 kb fragment in the ΔepcA strain (Fig. 5AB). The second PCR primer pair consisted of one for the sequences 0.1 kb (upstream) outside of the upstream fragment in pKO8542 and the other for the 5' region of the *npIII* cassette. This primer pair is supposed to yield 3.2 kb product only when pKO2542 is recombined into the chromosome, giving the $\Delta\text{epcA}::\text{npIII}$ genotype. This PCR displayed the expected 3.2 kb

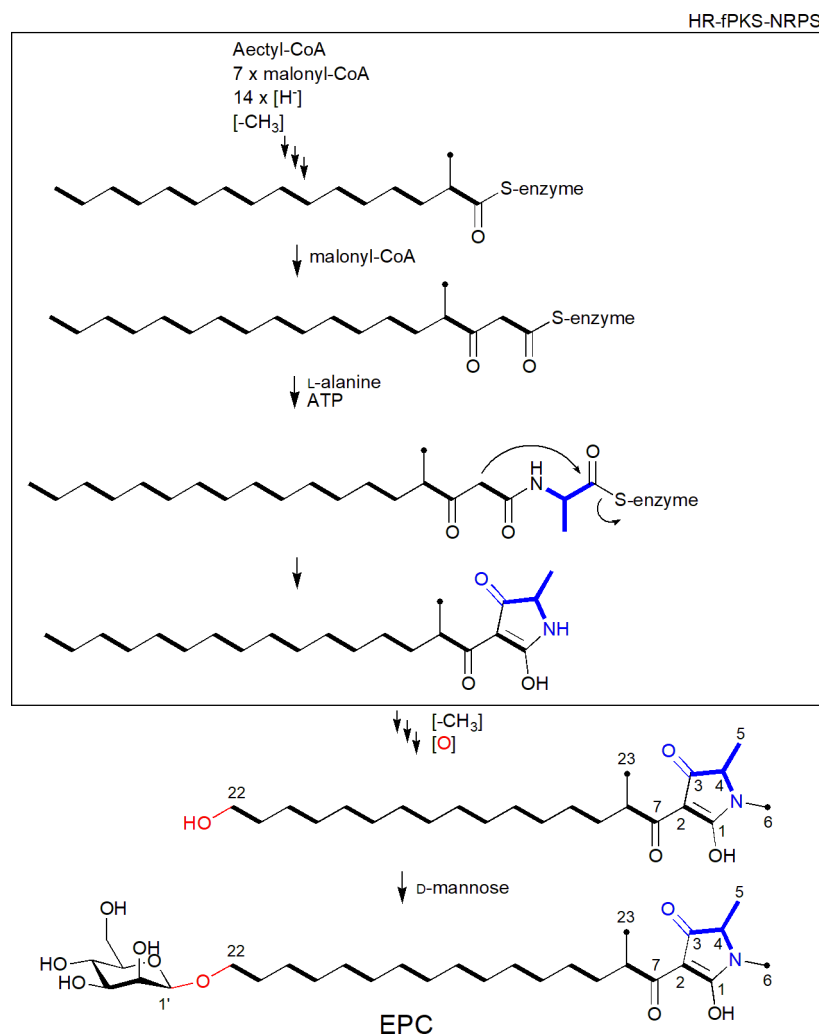


Fig. 3 The proposed biosynthetic pathway of EPC. The chain assembly steps of HR-fPKS-NRPS are shown in the box. It is hypothesized that the mannosylation is the final step of EPC biosynthesis, but it is ambiguous whether *N*-methylation precedes the mannosylation or not

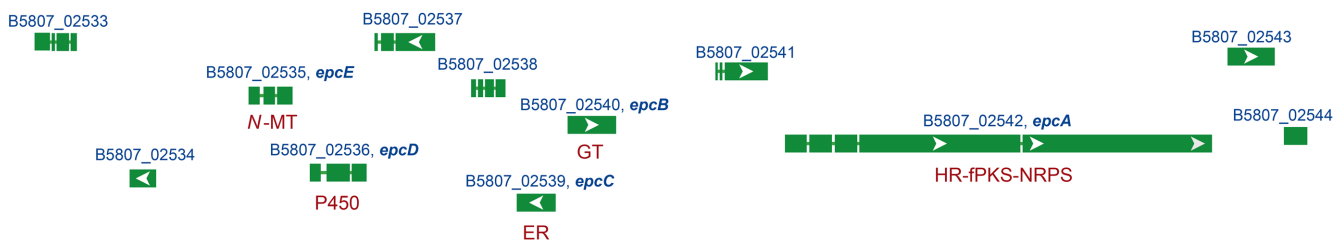


Fig. 4 The genetic organization of EPC BGC. The predicted enzyme functions were shown below the cognate genes, and the locus tags and the gene names were shown above. HR-fPKS-NRPS, highly reducing fungal polyketide synthase-nonribosomal peptide synthetase; GT, glycosyltransferase; ER, 2-enoylreductase; P450, cytochrome P450; *N*-MT, *N*-methyltransferase

product in the $\Delta epcA$ strain, whereas no signal was detected with WT DNA (Fig. 5AC). These PCR experiments demonstrate that the $\Delta epcA$ strain was successfully generated.

For *epcB* inactivation, a single PCR amplification can differentiate between WT and the $\Delta epcB::mptII$ genotype. The forward primer anneals at the 5' end of *epcB* and the reverse at 0.14 kb

downstream from the termination codon of *epcB*, which makes 1.5 and 3.3 kb product for WT and the $\Delta epcB$ strain, respectively (Fig. 6A). PCR analysis indicated the absence of a 1.5 kb product and presence of a 3.3 kb product in the $\Delta epcB$ strain (Fig. 6B), demonstrating that the inactivation of *epcB* was achieved.

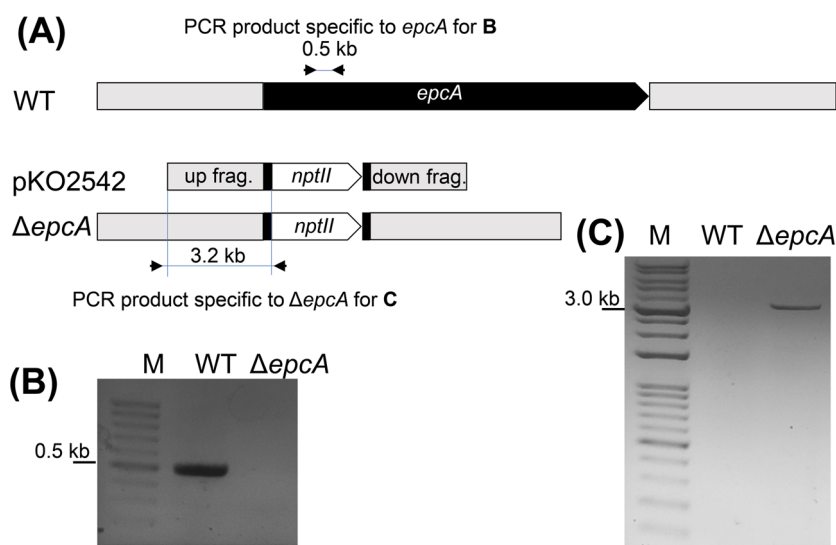


Fig. 5 Gene inactivation of *epcA*. (A) Gene inactivation scheme with the genetic map of *epcA*, the inactivation plasmid pKO2542, and the resulting inactivation mutant $\Delta epcA$. The sizes and positions of DNA products in the PCR experiments (B) and (C) are shown, which have been separated using agarose gel electrophoresis of the DNA product in the PCR amplification targeting the internal region of *epcA* (B) and targeting the recombinant DNA specific to $\Delta epcA::nptII$ (C). Lane M indicates the size marker that is composed of 0.1, 0.2, 0.3, 0.4, 0.5, 0.6, 0.7, 0.8, 0.9, 1.0, 1.5, 2.0, 3.0, 4.0, 5.0, 6.0, 8.0, and 10.0 kb fragment. Either the 0.5 kb (B) or 3.0 kb (C) is highlighted with a bar

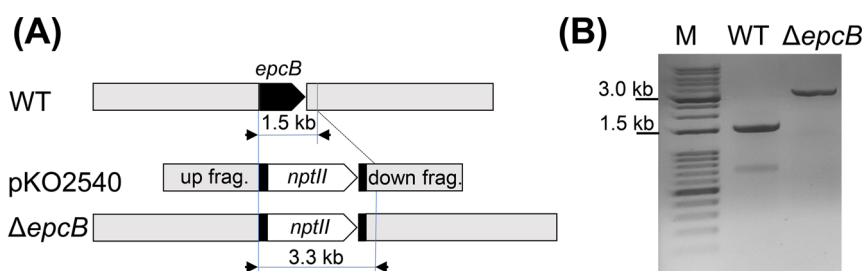


Fig. 6 Gene inactivation of *epcB*. (A) Gene inactivation scheme with the genetic map of *epcB*, the inactivation plasmid pKO2540, and the resulting inactivation mutant $\Delta epcB$. The sizes and positions of DNA products in the PCR experiment (B) are shown, which has been separated using agarose gel electrophoresis of the DNA product in the PCR amplification that differentiate *epcB* and $\Delta epcB::nptII$. (B) Lane M indicates the size marker that is composed of 0.1, 0.2, 0.3, 0.4, 0.5, 0.6, 0.7, 0.8, 0.9, 1.0, 1.5, 2.0, 3.0, 4.0, 5.0, 6.0, 8.0, and 10.0 kb fragment. The positions of 1.5 kb and 3.0 kb fragments are indicated with bars

Either *epcA* or *epcB* inactivation resulted in loss of EPC production

To assess EPC production in the $\Delta epcA$ and $\Delta epcB$ strains, both strains, together with WT, were cultured in YES liquid media, which afforded a high level of EPC production in WT. HPLC monitoring at 260 nm indicated that either the $\Delta epcA$ or $\Delta epcB$ strain was incapable of producing EPC (Fig. 7A). In this HPLC separation, the retention time of the minor isomer of OVT was close to that of the EPC. However, close inspection revealed that the positions of the two peaks were different. TLC analysis clearly showed that EPC was not found in the extracts of both $\Delta epcA$ and $\Delta epcB$ strains, whereas the presence of OVT was evident in them. This indicated that EPC production was selectively lost by the inactivation of either *epcA* or *epcB*.

Mannoylated acyltetramic acid BGC was previously reported

for burnetramic acid in *Aspergillus burnettii* [14]. Its tetramic acid moiety forms a pyrrolizidinedione structure with proline incorporation. Ectopic expression of burnetramic acid BGC in *Aspergillus nidulans* resulted in the production of burnetramic acid and its aglycone. This bolaamphiphilic compound, but not the aglycone, displayed antimicrobial activity. Considering this burnetramic acid biosynthesis study and the EPC biosynthetic pathway (Fig. 3), the absence of EPC aglycone in the $\Delta epcB$ strain is intriguing. It is possible that the EPC aglycone interferes with *E. nigrum* growth, and its secretion is limited, which hampers its accumulation inside the cell. There may be a feedback mechanism that inhibits its biosynthesis when mannosylation is absent. Acyltetramic acid compounds, such as melophins, are closely related to the EPC aglycone and display antimicrobial activity and cytotoxicity [15,16]. It may be worthwhile to explore the $\Delta epcB$

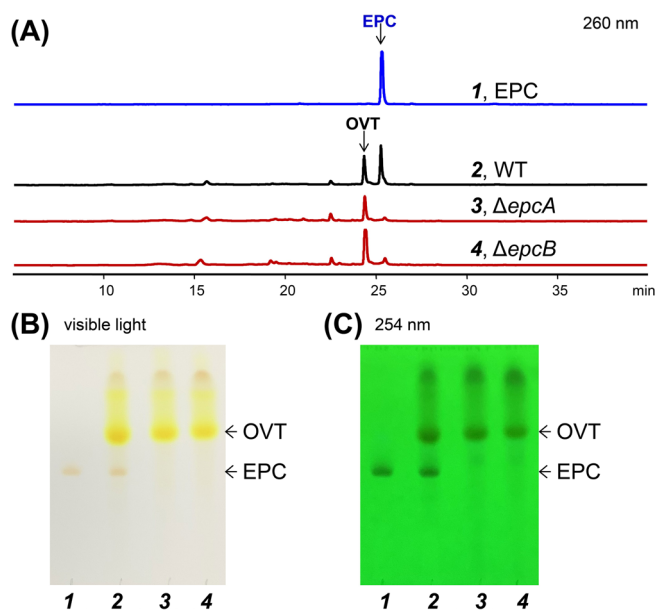


Fig. 7 Gene inactivation of either *epcA* or *epcB* resulted in selective loss of EPC production. (A) HPLC traces that were monitored at 260 nm are drawn to the same scale. The cell from the 50 mL YES culture was extracted with the same volume of methanol and 500 μ L of the extract was concentrated to 50 μ L, of which 20 μ L was applied. Eight micrograms of EPC were applied (1) and the elution (time) positions of OVT and EPC are indicated with arrows. All the traces. (B, C) TLC pictures captured under visible light (B) and under 254 nm UV light (C). EPC standard (1) and the extracts of WT (2), the $\Delta epcA$ (3), and $\Delta epcB$ (4) strain were applied

strain using various culture methods for EPC biosynthetic intermediate(s). Further gene inactivation studies to induce biosynthetic intermediate(s) may unveil the hidden biological activities of EPC.

Acknowledgment This research was supported by Basic Science Research Program through the National Research Foundation of Korea (NRF) funded by the Ministry of Education (NRF-2016R1D1A1B02009237).

References

1. Braga RM, Padilla G, Araújo WL (2018) The biotechnological potential of *Epicoccum* spp.: diversity of secondary metabolites. *Crit Rev Microbiol* 44: 759–778. doi: 10.1080/1040841X.2018.1514364
2. Fávoro LC, de Melo FL, Aguilar-Vildoso CI, Araújo WL (2011)

3. Polyphasic analysis of intraspecific diversity in *Epicoccum nigrum* warrants reclassification into separate species. *PLoS One* 6: e14828. doi: 10.1371/journal.pone.0014828
3. Fokin M, Fleetwood D, Weir BS, Villas-Boas S (2017) Genome sequence of the saprophytic ascomycete *Epicoccum nigrum* strain ICMP 19927, isolated from New Zealand. *Genome Announc* 5: e00557-17. doi: 10.1128/genomeA.00557-17
4. Cox RJ (2007) Polyketides, proteins and genes in fungi: programmed nano-machines begin to reveal their secrets. *Org Biomol Chem* 5: 2010–2026. doi: 10.1039/b704420h
5. Fisch KM (2013) Biosynthesis of natural products by microbial iterative hybrid PKS-NRPS. *RSC Adv* 3: 18228–18247. doi: 10.1039/C3RA42661K
6. Blin K, Shaw S, Steinke K, Villebro R, Ziemert N, Lee SY, Medema MH, Weber T (2019) antiSMASH 5.0: updates to the secondary metabolite genome mining pipeline. *Nucleic Acids Res* 47: W81–W87. doi: 10.1093/nar/gkz310
7. Medema MH, Kottmann R, Yilmaz P, Cummings M, Biggins JB, Blin K et al. (2015) Minimum information about a biosynthetic gene cluster. *Nat Chem Biol* 11: 625–631. doi: 10.1038/nchembio.1890
8. Lim YJ, Choi EH, Park SH, Kwon HJ (2020) Genetic localization of the orevactaene/epipyronone biosynthetic gene cluster in *Epicoccum nigrum*. *Bioorg Med Chem Lett* 30: 127242. doi: 10.1016/j.bmcl.2020.127242
9. Choi EH, Park SH, Kwon HJ (2021) Cytochrome P450 and the glycosyltransferase genes are necessary for product release from epipyronone polyketide synthase in *Epicoccum nigrum*. *J Appl Biol Chem* 64: 225–236. doi: 10.3839/jabc.2021.032
10. Hertweck C (2009) The biosynthetic logic of polyketide diversity. *Angew Chem Int Ed Engl* 48: 4688–4716. doi: 10.1002/anie.200806121
11. Namiki F, Matsunaga M, Okuda M, Inoue I, Nishi K, Fujita Y, Tsuge T (2001) Mutation of an arginine biosynthesis gene causes reduced pathogenicity in *Fusarium oxysporum* f. sp. *melonis*. *Mol. Plant Microbe Interact.* 14: 580–584. doi: 10.1094/MPMI.2001.14.4.580
12. Wright AD, Osterhage C, König GM (2003) Epicoccamide, a novel secondary metabolite from a jellyfish-derived culture of *Epicoccum purpurascens*. *Org Biomol Chem* 1: 507–510. doi: 10.1039/b208588g
13. Wangun HV, Dahse HM, Hertweck C (2007) Epicoccamides B-D, glycosylated tetramic acid derivatives from an *Epicoccum* sp. associated with the tree fungus *Pholiota squarrosa*. *J Nat Prod.* 70: 1800–1803. doi: 10.1021/np070245q
14. Li H, Gilchrist CLM, Lacey HJ, Crombie A, Vuong D, Pitt JI, Lacey E, Chooi YH, Piggott AM (2019) Discovery and heterologous biosynthesis of the burnettramic acids: Rare PKS-NRPS-derived bolaamphiphilic pyrrolizidinediones from an Australian fungus, *Aspergillus burnettii*. *Org Lett.* 21:1287–1291. doi: 10.1021/acs.orglett.8b04042
15. Wang CY, Wang BG, Wirjowidagdo S, Wray V, van Soest R, Steube KG, Guan HS, Proksch P, Ebel R (2003) Melophlins C-O, thirteen novel tetramic acids from the marine sponge *Melophlus sarassinorum*. *J Nat Prod.* 66:51–56. doi: 10.1021/np0202778
16. Xu J, Hasegawa M, Harada K, Kobayashi H, Nagai H, Namikoshi M (2006) Melophlins P, Q, R, and S: four new tetramic acid derivatives, from two Palauan marine sponges of the genus *Melophlus*. *Chem Pharm Bull (Tokyo).* 54:852–854. doi: 10.1248/cpb.54.852